Artvin Çoruh Üniversitesi
Doğal Afetler Uygulama ve Araştırma Merkezi
Doğal Afetler ve Çevre Dergisi

Artvin Çoruh University
Natural Hazards Application and Research Center
Journal of Natural Hazards and Environment

Araştırma Makalesi / Research Article, Doğ Afet Çev Derg, 2026; 12(2): 442-454, DOI: 10.21324/dacd.1837184

Investigation of the Efficiency of Biochar and Activated Carbon Produced from Water Hyacinth and Phragmites Australis Plants

Ahmed Abboosh[1,*], Semra Çoruh[1]

[1]*Ondokuz Mayıs University, Faculty of Engineering, Department of Environmental Engineering, 55000, Samsun, Türkiye*

Abstract

This study examined how varying pyrolysis temperatures influence the formation of biochar and activated carbon derived from Phragmites australis and Eichhornia crassipes. The work assessed changes in mass yield, surface area, and pore development resulting from thermal decomposition and chemical activation using potassium hydroxide (KOH). Pyrolysis was conducted under strictly oxygen-free conditions using nitrogen gas at 500, 550, and 650 °C, with a heating rate of 10 °C/min and a residence time of 90 minutes. Biochar yield for both feedstocks declined progressively at higher temperatures because of intensified volatilization and structural mass loss. Water hyacinth produced its maximum yield at 550 °C(CHN550), reaching 25.8%, whereas the value decreased to 22.6% at 650 °C. P. australis exhibited a yield of 24.4% at 500 °C(CHS500), falling to 21% at 650 °C. For activated carbon, the highest output was recorded for P. australis at 550 °C(ACS550), at 23.6%, dropping to 17.6% at 650 °C. Water hyacinth showed the lowest yield at 650 °C(ACN650), at 14.6%. In contrast, surface characteristics improved markedly at elevated temperatures. BET results showed increased surface area and enhanced microporosity, especially after activation. The (ACS650) sample reached 196.69 m²/g, while (ACN650) achieved an even greater surface area of 252.95 m²/g.

Keywords
Water Hyacinth, Phragmites Australis, Activated Carbon, Biochar

Su Sümbülü ve Saz Bitkilerinden Üretilen Biyokömür ve Aktif Karbonun Etkinliğinin İncelenmesi

Özet

Bu çalışma, saz ve su sümbülü bitkilerinden elde edilen biyokömür ve aktif karbon üretimi üzerinde piroliz sıcaklıklarının etkisini incelemiştir. Araştırma kapsamında, potasyum hidroksit (KOH) ile yapılan kimyasal aktivasyon ve piroliz süreçlerinin kütle verimi, yüzey alanı ve gözenek yapısı üzerindeki etkileri değerlendirilmiştir. Piroliz, oksijensiz ortamda ve azot gazı altında 10 °C/dak ısıtma hızı ve 90 dakikalık bekletme süresiyle 500, 550 ve 650 °C'de gerçekleştirilmiştir. Artan sıcaklık, uçucu bileşen kaybının hızlanması nedeniyle her iki bitkide biyokömür veriminde düşüşe yol açmıştır. Su sümbülü 550 °C'de %25,8 (CHN550) ile en yüksek verimi gösterirken, 650 °C'de verim %22,6'ya gerilemiştir. Saz ise 500 °C'de %24,4 (CHS500) verim sağlamış ve 650 °C'de bu değer %21'e düşmüştür. Aktif karbon üretiminde en yüksek verim, 550 °C'de %23,6 ile saz örneğinde (ACS550) elde edilmiş; 650 °C'de %17,6'ya inmiştir. Su sümbülünde 650 °C'de en düşük verim (ACN650) %14,6 olarak kaydedilmiştir. Yüzey özellikleri ise sıcaklıkla belirgin biçimde iyileşmiş; özellikle aktive örneklerde BET yüzey alanı ve mikrogözeneklilik artmıştır. Saz (ACS650) örneği 196,69 m²/g yüzey alanına ulaşırken, su sümbülü (ACN650) aynı sıcaklıkta 252,95 m²/g ile daha yüksek bir değer göstermiştir.

Anahtar Sözcükler
Su Sümbülü, Saz Bitkisi, Aktif Karbon, Biyokömür

1. Introduction

The production of highly porous carbonaceous materials such as biochar and activated carbon has become a central field in wastewater and industrial effluent treatment, environmental pollution control, and the development of efficient sorbent materials (Thompson et al., 2016). Biochar is produced by thermally decomposing biomass in the absence of oxygen. This process yields a carbon-rich solid with stable structure and adjustable properties (Madej et al., 2016). Activated carbon represents a more advanced form of such materials; it undergoes additional physical and chemical transformation steps that create an intricate network of fine pores and reactive surface sites. These steps enhance substantially enhances its capacity to capture both organic and inorganic contaminants (Jeirani et al., 2017; Colomba et al., 2022). The production techniques and process variables such as temperature, heating rate, time, gas environment, and raw material types are the basic determinates of the yiels and characteristics of biochar and activated carbon. Among the parameters influencing the

* Corresponding Author: Tel: +90 (362) 312 1919
E-mail: 21281190@stu.omu.edu.tr (Abboosh A), semcoruh@omu.edu.tr (Çoruh S)
Gönderim Tarihi / Received : 06/12/2025
Kabul Tarihi / Accepted : 08/06/2026

characteristics of these carbon materials, temperature plays a decisive role. It governs the breakdown of organic constituents, the release of volatile fractions, the evolution of pore systems, and the structural rearrangements within the carbon matrix. During the initial stages of pyrolysis, higher temperatures promote the removal of functional groups and the cleavage of weaker chemical bonds. After that the stages of pyrolysis facilitating the reorganization of aromatic domains and the expansion or collapse of pores depending on the precursor biomass and preparation pathway (Novotny et al., 2015; Hagemann et al., 2018; Zhang, Shao, et al., 2020a). The influence of temperature becomes even more pronounced during chemical activation processes (Azargohar & Dalai, 2006) particularly those employing potassium hydroxide (KOH) where strong alkaline agents interact with the carbon framework to generate internal channels and large pore volumes (macropores or mesopores), thereby significantly improving the textural and surface properties of the final product (Azargohar & Dalai, 2008; Hui & Zaini, 2015; Williams et al., 2022). For this reason, systematic investigation of thermal conditions is essential for elucidating the relationship between pyrolysis parameters and the resulting physicochemical features, especially with respect to surface area, pore volume, and mass yield (Gale et al., 2021). Such studies acquire added importance when utilizing rapidly growing aquatic plants, including Phragmites australis and Water hyacinth (Eichhornia crassipes), as sustainable, low-cost, and readily convertible feedstocks for producing carbon materials suitable for a wide range of industrial applications (Masto et al., 2013).

The cosmopolitan distribution of Phragmites australis is well documented, although its precise point of origin remains uncertain. Its native range is believed to span broad regions of Africa, in addition to large parts of Europe, northern and western Asia, North and Central America, South America, and northern and eastern Australia. Numerous studies confirm the plant's widespread presence across wetland ecosystems worldwide (Chen et al., 2024). Phragmites australis is a perennial, tall, herbaceous species capable of forming expansive stands, reaching heights between 4 and 6 meters. This growth habit is supported by an extensive network of subterranean rhizomes that enable rapid vegetative propagation and the establishment of dense reed beds. Reproduction occurs through both seed dispersal facilitated by wind and water and through horizontally spreading stems that root upon contact with suitable substrates. Under favorable environmental conditions, the plant can achieve annual growth increments of up to 5 meters. Its ability to withstand elevated salinity, waterlogged soils, and acidic sulfate-rich substrates contributes to its competitive dominance in disturbed landscapes. Monospecific stands of Phragmites australis can significantly alter hydrological dynamics and wildlife habitats, while the accumulation and subsequent die-off of tall stems increase the likelihood of fire events. For the production of activated carbon, researchers often prefer the stems over leaves or roots.

The stems possess relatively high cellulose and lignin contents, minimal ash and impurities, and a more cohesive fiber structure, all of which support the formation of stable and well-developed porous frameworks during pyrolysis. Their inherent resistance to thermal degradation also allows for better control over carbonization conditions. Therefore, stems were used in this study, as seen in Figure 1 below. From a morphological standpoint, Phragmites australis exhibits erect, hollow culms measuring approximately 150–600 cm in length and 5–15 mm in diameter. These culms display a brown, ribbed exterior and are accompanied by broad, pointed leaves ranging from 15 to 60 cm long and 1 to 6 cm wide. Its inflorescences consist of dense, fine panicles grayish or purple in appearance measuring 15–40 cm in length and blooming between July and October. The plant produces small, lightweight brown seeds that are typically around 8 mm long (Chambers et al., 1999; Rolletschek et al., 1999; Saltonstall, 2002; Shengli et al., 2018).

Figure 1: Stems of Phragmites australis plant

Eichhornia crassipes, commonly known as the water hyacinth, is an aquatic plant whose native range lies within the Amazon Basin of South America. Over the past decades, however, it has expanded far beyond its original habitat and has become established across numerous tropical and subtropical regions worldwide. Among the countries where it spread most including the United States, Egypt, India, and Australia. One of the main reasons for its spread largely as a result of its intentional introduction as an ornamental species (Toft et al., 2003; Zhang et al., 2010). The plant was introduced into Iraq during the 1980s for decorative purposes and is now widely observed along the banks of major rivers (Abdulrazzak, 2017; Al-Kinani & Mana, 2024). Its invasive behavior has been documented in more than fifty countries, a pattern strongly linked to human activities such as the aquarium trade, which have accelerated its global dissemination. Water hyacinth grows rapidly as a floating, perennial hydrophyte, and under optimal environmental conditions its population

can double within approximately two weeks. It reproduces both sexually and vegetatively; the plant generates thousands of seeds each year, capable of remaining viable for up to thirty years, in addition to stolon-like structures that give rise to new daughter plants. The growth performance of Eichhornia crassipes is influenced by multiple environmental parameters, particularly water acidity and temperature.

It thrives in water with a pH between 6 and 8 and can tolerate temperatures approaching 40 °C. Understanding the physical and chemical attributes of this species is essential for evaluating its ecological significance and its potential industrial applications. The plant exhibits thick, waxy, oval-shaped leaves typically 10 to 20 cm in diameter supported by buoyant, spongy petioles that enable it to float. Water hycainth used in this study was seen in Figure 2.

Figure 2: Water hyacinth

Its root system consists of fibrous, feather-like structures that are dark purple to nearly black, with fine white root hairs. Mature individuals range in height from approximately 40 cm to 1 m and may produce up to ten flowers per plant (Rezania et al., 2015; Gaurav et al., 2020). Table 1 shows the thermal conditions that were chosen for the preparation of biochar in some of the literature.

Table 1: Phragmites australis and water hyacinth as feedstocks for biochar preparation

Feedstock	Preparation condition	Carbon content %	References
Phragmites australis	Pyrolysis 600 °C, 1hr	76.46	(Gong et al., 2017)
Modified biochar Phragmites australis	Pyrolysis 600 °C, 1hr	54.35	(Gong et al., 2017)
Phragmites australis	Pyrolysis, 500 °C, 60 min	65.46	(Jiang et al., 2022)
Phragmites australis	Pyrolysis, 823 °C, 30 min	-	(Sharifirad M et al., 2012)
Mixture of Waterworks sludge & phragmites australis	Pyrolysis 600 °C, 50 min	57.78	(Zhao et al., 2020)
Waterworks sludge	Pyrolysis 400 °C, 30 min	37.35	(Zhao et al., 2020)
Eichhornia crassipes (water hyacinth)	Pyrolysis 450 °C, 60 min	32.80	(Najmudeen et al., 2019)
Eichhornia crassipes (water hyacinth)	Pyrolysis 350 °C, 40 min	64.11	(Masto et al., 2013)
Eichhornia (water hyacinth)	Pyrolysis 700 °C, 120 min	-	(Salman et al., 2021)
Water hyacinth	Pyrolysis 600 °C, 120 min	-	(Tarapitakcheevin et al., 2013)
Water hyacinth leaves	Pyrolysis 400 °C, 60 min	-	(Riyanto & Prabalaras, 2019)

This study examines how selected pyrolysis temperatures (500, 550, and 650 °C) influence the yield of biochar and activated carbon derived from two aquatic plant species. It aims to identify thermal conditions that balance carbon yield and pore development, enabling the production of efficient porous adsorbents for wastewater treatment. A direct comparison is established between Phragmites australis and Eichhornia crassipes (Water Hyacinth) under identical experimental conditions, allowing a clear assessment of temperature effects within a unified framework. In addition, chemical activation using potassium hydroxide (KOH) was applied under controlled conditions to evaluate structural evolution across different temperatures. The results further reveal a relationship between decreasing yield and increasing surface area, providing insight into optimizing carbon material production from aquatic biomass.

2. Materials and Methods

2.1. Raw Materials

In this study, Water hyacinth and Phragmites australis were employed as biomass precursors. The plant samples were collected from the banks of the Tigris River in the Al-Zab district of Kirkuk Province, Iraq. Following collection, the materials underwent an initial cleaning stage to remove clay residues and other impurities using water, after which they were left to dry naturally under sunlight (Carneiro et al., 2023). The dried plants were subsequently cut into small fragments with an average size of approximately 1-2 mm (Sharifirad M et al., 2012; Huang et al., 2014). To ensure complete moisture removal and to preserve the internal structural integrity of the biomass, the material was further dried

in a laboratory oven at 60 °C for 24 hours (Liao et al., 2011; Orero et al., 2025). The experimental work incorporated a set of laboratory instruments and materials, including a Saftherm Sante furnace (30–3000 °C), an NG-300P nitrogen generator, purified KOH pellets (S D Fine-Chem Limited), a Faithful drying oven, deionized water for washing, and a Value VE115N vacuum pump to facilitate the washing process. Additional preparation steps involved grinding the material with a porcelain mortar, sieving through a 60-mesh screen, and characterizing the resulting carbon materials using a 3Flex BET surface area analyzer (version 6.02). The preparation of carbon materials in this study was carried out based on controlled laboratory procedures developed according to commonly applied approaches in biomass conversion studies. The experimental conditions were carefully designed to ensure consistent thermal treatment and reliable formation of carbon structures.

Biomass drying, size reduction, pyrolysis, chemical activation steps were performed under well-defined conditions using standard laboratory equipment. The drying stage was conducted to remove residual moisture and stabilize the raw material prior to thermal processing. The pyrolysis process was carried out in an oxygen-limited environment with continuous nitrogen flow to prevent oxidation and to promote carbonization (Peixoto et al., 2020).

2.2. Preparation of Water Hyacinth (CHN) and Phragmites Australis (CHS) Biochar

The preparation steps were carried out following widely reported procedures in biomass carbonization studies, with minor adjustments according to the experimental setup. After drying the samples, 5 g of each biomass were weighed and placed in a Saftherm Pyrolysis furnace. In absence of oxygen, the pyrolysis was performed with N_2 gas passed through at a constant flow rate of 230 mL/min. A heating rate of 10 °C/min was used, and the heat fixation time was 90 minutes at three selected Pyrolysis temperatures: 500, 550, and 650 °C. After the process, the samples were left to cool inside the furnace, washed with deionized water, and dried at 105 °C for 24 hours. Subsequently, the samples were ground using a ceramic mortar and sieved through a 60 mesh sieve (Xu et al., 2020; Narayanan et al., 2021; Hadey et al., 2022; Hadey et al., 2022; Hung et al., 2023). The symbols used are: CHS for biochar extracted from Phragmites australis and CHN for biochar extracted from water hyacinth. Figure 3, show Stages of biochar production from Phragmites australis and water hyacinth (Eichhornia crassipes).

Grinding and washing stage of the Phragmites australis plant

Grinding and washing stage of the water hyacinth plant

The biochar was obtained from Phragmites australis and water hyacinth, then ground and sieved at a 60 mesh.

Figure 3: Stages of obtaining biochar from Phragmites australis and water hyacinth (Eichhornia crassipes).

2.3. Preparation of Water Hyacinth (ACN) and Phragmites Australis (ACS) Activated Carbon

The preparation steps were carried out following widely reported procedures in production of activated carbon studies studies, with minor adjustments according to the experimental setup. The use of potassium hydroxide KOH in the production or activation of activated carbon gives higher surface areas compared to other chemicals such as phosphoric acid H_3PO_4 or zinc chloride $ZnCl_2$ (Elmouwahidi et al., 2017; Ma, 2017; Saad et al., 2020; Harimisa et al., 2022; Ullah et al., 2024). Biomass was chemically activated using a 20% potassium hydroxide solution at a mass ratio of 1 plant:3 KOH (Williams et al., 2022). Samples were soaked in the solution for 24 hours, and then dried at 105°C for another 24 hours. After drying, 5 grams of each sample were weighed and pyrolysis in a Saftherm furnace under the same temperature conditions used for biochar production (500, 550, and 650°C) in the presence of N_2 gas (Okman et al., 2014). After Pyrolysis, the materials were washed with deionized water using a vacuum pump to accelerate the removal of residual KOH. The washing process continued until the pH reached 7 (Ahmed & Theydan, 2012). Finally, the samples were dried at 105°C for 24 hours, then ground and sieved through a 60 mesh sieve. The same KOH-based chemical activation approach was applied to both biomass types in order to maintain identical preparation conditions and enable a direct and reliable comparison between the resulting carbon materials, following established procedures reported in the literature (Khalil et al., 2013). The following symbols were adopted: ACS for activated carbon prepared from Phragmites australis and ACN for activated carbon prepared from water hyacinth.

In addition to the grinding, washing, and drying stages mentioned earlier in the biochar production process, the following stage shows the preparation of a potassium hydroxide solution, its mixing with the plants using a blender, and its incubation for 24 hours. Figure 4, show stages of activated carbon production from Phragmites australis and water hyacinth.

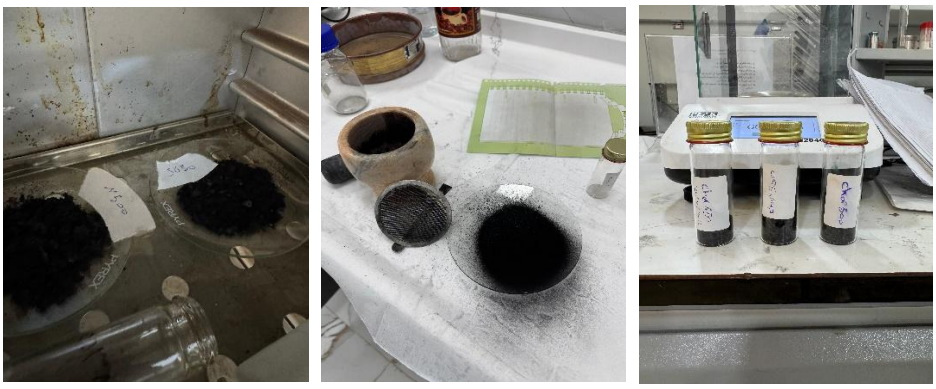

Drying stage after washing, followed by grinding and sieving using a 60 mesh sieve

Figure 4: Stages of obtaining activated carbon from Phragmites australis and water hyacinth

2.4. Effect of Pyrolysis Temperature Assessment

The effect of pyrolysis temperatures (500–650 °C) on biochar and activated carbon yield and pore structure development. The same operating conditions were used for all samples to ensure accurate comparison between temperature and the two plant species.

2.5. Yield Determination

The mass yield for each sample was calculated using the formula (Adesina et al., 2021):

$$\text{Yield}_{\text{(Biochar \& activated carbon)}}(\%) = \frac{\textbf{\textit{Mass of Carbon Produced (g)}}}{\textbf{\textit{Mass of Dry Biomass (g)}}} \times 100 \quad (1)$$

The calculation was performed for all temperatures and for each of the CHS, CHN, ACS, and ACN samples.

2.6. Surface Area and Porosity Analysis

The 3Flex BET Version 6.02 instrument was used to determine: Specific surface area using the BET method and Pore size and distribution, as needed. Analysis was performed on all samples after drying and sieving to ensure homogeneity.

3. Results and Discussion

3.1. Biochar Yield

Many studies and laboratory research conducted on this topic (biochar and activated carbon production and yield) have indicated and proven that the yield decreases in quantity with increasing temperatures (Nwajiaku et al., 2018; Zhang, Zhang, et al., 2020b; Adesina et al., 2021). Multiple biochar samples were produced from both plant species: water hyacinth and Phragmites australis, with three samples prepared for each plant. These samples were subjected to pyrolysis at three different temperatures: 500 °C, 550 °C, and 650 °C. The biochar yield was determined according to the following equation:

$$\text{Yield}_{\text{(Biochar)}}(\%) = \frac{\textit{Mass of Carbon Produced (g)}}{\textit{Mass of Dry Biomass (g)}} \times 100 \quad (2)$$

Biochar yield is an indicator that reflects the efficiency of the thermal conversion process. This yield depends on several factors, including the type of raw biomass, the pyrolysis temperature, the pyrolysis duration, and the heating rate. Generally, as the temperature increases, the biochar yield decreases (Ouyang et al., 2020), while both the carbon content and the specific surface area tend to increase. As we see in table 2.

Table 2: Comparison of BiocharYield from Different Biomass under Various Pyrolysis Conditions

P. australis	Pyrolysis Temperature (˚C)	Time (min)	Yield %	Ref.	Water hyacinth	Pyrolysis Temperature (˚C)	Time (min)	Yield %	Ref.
CHS 500	500	90	24.4	This work	CHN 500	500	90	24.4	This work
CHS 550	550	90	23.6	This work	CHN 550	550	90	25.8	This work
CHS 650	650	90	21	This work	CHN 650	650	90	22.6	This work
Biochar	600	60	27.59	(Gong et al., 2017)	Biochar	500	90	10	(Masto et al., 2013)
Modified Biochar	600	60	50.55	(Gong et al., 2017)	Biochar	500	30	20	(Masto et al., 2013)
Biochar	300	120	50.19	(Wang et al., 2021)	Biochar	400	90	15	(Masto et al., 2013)
Biochar	500	120	28.99	(Wang et al., 2021)	Biochar	400	30	28	(Masto et al., 2013)
Biochar	500	60	33.37	(Xiao et al., 2022)	Biochar	300	40	44.6	(Kassa et al., 2025)
Biochar	300	60	29.5	(Liu et al., 2016)	Biochar	350	20	33.6	(Narayanan et al., 2021)
Biochar	500	60	16.5	(Liu et al., 2016)	Biochar	500	20	23	(Narayanan et al., 2021)

To support the interpretation of biochar yield, data from multiple published studies were compiled and compared with the present results, as shown in Table 2. The values obtained for both P. australis and water hyacinth at 500–650 °C fall within the range reported in earlier work, indicating that the applied conditions are consistent with established practices. A gradual decrease in yield with increasing temperature is clearly observed in this study, which agrees with the general trend reported in the literature (Ouyang et al., 2020). This behavior is mainly related to the progressive release of volatile compounds and the increased degree of thermal decomposition at higher temperatures.

However, some variations can be seen when comparing different studies. For example, higher yields reported at lower temperatures or longer residence times may be attributed to reduced thermal severity or differences in biomass composition. In contrast, lower yields observed in certain cases may result from shorter processing times or more intensive devolatilization. The relatively higher yield of modified biochar in some studies can also be linked to the presence of inorganic components that remain within the solid structure after thermal treatment.
Overall, the comparison confirms that the yield values obtained in this work are reasonable and fall within the expected range. It also highlights that temperature, time, and biomass characteristics play a combined role in determining the final yield.

3.2. Activated Carbon Yield

Studies have indicated that the use of potassium hydroxide in the production of activated carbon increases the surface area and improves the adsorption properties of activated carbon produced from various organic materials, in addition to a good yield in some applications (Li et al., 2018).
Several activated carbon samples were produced from both plant species: Water hyacinth and Phragmites australis, with three samples prepared from each plant. The samples were subjected to pyrolysis under direct chemical activation at three different temperatures: (500 °C, 550 °C, and 650 °C) As we see in Table 3. The activated carbon yield was calculated according to the following equation:

$$\text{Yield}_{\text{activated carbon}}\ (\%) = \frac{Mass\ of\ Carbon\ Produced\ (g)}{Mass\ of\ Dry\ Biomass\ (g)} \times 100 \quad (3)$$

Table 3: Effect of Activation Temperature and Residence Time on Activated Carbon Yield from Various Biomass Sources

Precursors	Pyrolysis Temperature (°C)	Time (min)	Activating Reagent	Activated Carbon Yield %	Ref.
P. Australis	500	90	KOH	21.6	This Work
P. Australis	550	90	KOH	23.6	This Work
P. Australis	650	90	KOH	17.6	This Work
Water Hyacinth	500	90	KOH	21	This Work
Water Hyacinth	550	90	KOH	19.4	This Work
Water Hyacinth	650	90	KOH	14.6	This Work
Grape Seeds	600	60	KOH	33.2	(Okman et al., 2014)
Grape Seeds	800	60	KOH	30.5	(Okman et al., 2014)
Spent mushroom compost	500	105	KOH	20	(Ullah et al., 2024)
Cane pith	780	60	KOH	8.2	(Tseng & Tseng, 2006)
Rice straw	800	60	KOH	13.5	(Basta et al., 2009)
Coconut shell	700	90	NaOH	18.8	(Cazetta et al., 2011)
Eucalyptus bark	500	60	H_3PO_4	26	(Patnukao & Pavasant, 2008)
Date palm pits	450	72	H_3PO_4	41.0	(Reddy et al., 2012)
Vetiver roots	600	60	H_3PO_4	48	(Altenor et al., 2009)
Date stones	500	72	$ZnCl_2$	40.4	(Ahmed & Theydan, 2012)
Waste tea	800	120	$C_2H_3O_2K$	27.9	(Ullah et al., 2024)
Paper mill sludge	800	150	K_2CO_3	3.4	(Ahmed, 2016)

To provide a clearer interpretation of the obtained results, data from different biomass sources reported in previous studies were compiled and compared with the present work, as summarized in the table. The comparison includes various precursor types, activation agents, temperatures, and residence times. The collected data show that the yield of activated carbon is strongly influenced by both thermal conditions and the nature of the raw material.
In general, higher activation temperatures tend to reduce the final yield due to the intensified release of volatile matter and the progression of carbon burn-off. At the same time, longer residence times may further decrease the solid fraction as thermal reactions continue within the carbon matrix. However, this trend is not identical for all materials. Variations in lignocellulosic composition, ash content, and structural properties lead to noticeable differences in yield even under similar conditions. The comparison also indicates that the yields obtained from P. australis and water hyacinth fall within the range reported for other biomass precursors treated with chemical activation. This confirms that the selected preparation conditions are suitable and produce results consistent with those found in the literature. Overall, the combined effect of temperature, activation time, and precursor characteristics plays a decisive role in determining the final yield of activated carbon.
Figure 5 shows that plant species, temperature, and preparation method clearly influence the amount of biochar and activated carbon produced. The results show that Water hyacinth outperforms Phragmites australis in solid carbon production across all temperatures, both in its unactivated state and after chemical activation, reflecting the suitability of its cellular structure for retaining greater mass after pyrolysis. It is also evident that increasing temperature consistently leads to a decrease in yield across all samples, a behavior associated with increased decomposition of volatile components and loss of solid mass under elevated thermal conditions. This is accompanied by a higher yield of biochar compared to activated carbon, as the chemical activation process using KOH removes part of the carbon structure during pore

formation, which explains the additional decrease in final mass. By comparing the temperatures, it appears that each plant and each carbon species has an optimal temperature for achieving the highest yield. The best yield of biochar is achieved at 500 °C by the Phragmites australis, while the highest productivity is reached at 550 °C by the water hyacinth. The highest yields of activated carbon vary between 500 and 550 °C depending on the plant. These results allow us to understand the general trends in the behavior of the raw material during pyrolysis, identify the most efficient thermal conditions for producing high-yielding solid carbon, and provide a scientific explanation for the inverse relationship between increasing temperature and decreasing yield. This supports the use of this scheme as an analytical tool for interpreting experimental results and further explores the impact of temperature and chemical activation on the properties of the produced carbon materials.

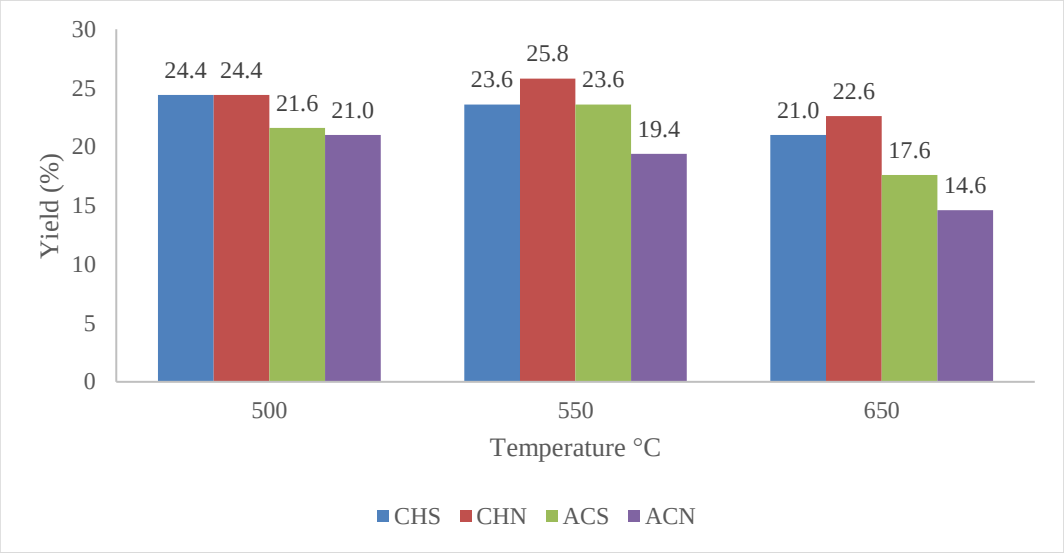

Figure 5: Comparison of biochar and activated carbon yields of Phragmites australis and water hyacinth at different Pyrolysis temperatures

3.3. BET Results and Porous Structure

BET data reveal a clear variability in the response of both the raw material and its interaction with the processing method (simple carbonization vs. chemical activation) and the degree of pyrolysis. In general, three main characteristics emerge from the results: the qualitative difference between plants as a biomass source, the effect of chemical activation on increasing the total surface area and developing micropores, and the effect of temperature as a catalyst or decreaser of surface area depending on the combination of conditions.

First, for unactivated biochar, measurements reveal that reed ore yielded significantly higher specific surface areas compared to water hyacinth at the same pyrolysis degrees. For example, the Phragmites australis sample carbonized at 500 °C recorded a relatively high BET value (approximately 136.36 $m^2 \cdot g^{-1}$), while the BET value of water hyacinth at 500 °C was very low (~25.03 $m^2 \cdot g^{-1}$). This difference indicates a fibrous structure more capable of retaining larger surface areas after pyrolysis in the Phragmites australis, a predictable result of variations in texture (cellulose, lignin and ash ratio) that influence the precursor's resistance to Pyrolysis and pore formation pattern.

Secondly, the effect of chemical activation using KOH is clear and significant: activated samples showed a marked increase in BET compared to their unactivated counterparts, with considerable variation depending on the raw material and degree of Pyrolysis. For example, activated carbon derived from reeds at 650 °C yielded the highest BET values among the samples (≈196.70 $m^2 \cdot g^{-1}$), while other activated water hyacinth samples also showed high values at medium/high temperatures (e.g., the BET value of ACN samples reached high levels at 550–600 °C, with a very high value observed at 600 °C in the coil, showing a continuous increase with increasing temperature up to a certain limit. This supports the idea that the reaction of KOH with the carbon structure at high temperatures opens up a microporous network and generates a large internal surface by removing some of the carbon and forming microporous pathways (micropores).

Third, the relationship between temperature and surface area is not linear, and this applies only to the raw material. While BET increased in several activated samples as the Pyrolysis temperature was raised to 650 °C (especially in activated reed), unactivated water hyacinth carbons showed little increase or stability when moving from 550 to 650 °C. This suggests that increasing the temperature can, in some cases, lead to a reorganization of the carbon structure (aromatic condensation), which limits the surface area or destroys fragile pores formed at lower temperatures. In other words, temperature acts as a dual agent: at reasonable levels, it accelerates the action of chemical abrasives and forms micropores, while at much higher levels, it can contribute to the melting or shrinkage of previously formed micropores.

Regarding pore size and distribution data, the t-Plot, BJH, and D-H data in the file indicate an increase in the total pore size and the proportion of micropores in the activated samples at higher temperatures. An increase in the combined values of pore volumes (BJH cumulative volume & single-point total pore volume) was observed, paralleling the increase in BET in these samples. This indicates that the increase in BET is not solely due to an increase in surface area, but is also associated with a genuine growth in micro and intermediate porosity, properties that enhance the material's molecular adsorption capacity and environmental applications. Furthermore, observations of the Horvath-Kawazoe and Dubinin-Astakhov curves in the profile show a clear expansion in micropore volume after chemical activation, particularly in the high-temperature activated Phragmites australis samples.

From a comparative performance perspective, it can be concluded that Phragmites australis is the best raw material for producing (high-surface-area) carbon after chemical activation at 650 °C. While water hyacinth exhibits good potential for higher initial yields at intermediate temperatures (as indicated by the yield data in the profile), its specific surface area remains lower compared to activated Phragmites australis. This variation introduces a range of practical considerations: if the priority is surface area and microporosity (e.g., for molecular adsorption of phenols or heavy metals), then it is best to choose a reed activated at a high temperature; if the priority is material/economic efficiency in terms of yield, then water hyacinth may be useful at a medium temperature with economic activation.

Finally, the interrelationship between yield and surface area points to a clear practical trade-off: higher porosity and surface area often come at the expense of lower yield, especially after chemical activation and increased temperature. Therefore, the choice of manufacturing conditions requires a balance between application requirements (high surface area versus product cost/quantity). In the Table 4 below, the results of the BET- surface area analysis are summarized.

Table 4: BET results for biochar and activated carbon samples produced from Water hyacinth and Phragmites Australis plants at different temperatures

Sample	Temp (°C)	BET Surface Area (m^2/g)	Total Pore Volume (cm^3/g)	Avg. Pore Diameter (nm)
CHS500	500	136.36	0.18084	5.3
CHS550	550	130.63	0.1632	4.99
CHS650	650	166.91	0.21614	5.18
CHN500	500	25.03	0.04219	6.74
CHN550	550	43.02	0.06841	6.36
CHN650	650	44.59	0.06926	6.21
ACS550	550	60.84	0.09885	6.49
ACS650	650	196.7	0.26435	5.38
ACN500	500	129.37	0.19167	5.93
ACN550	550	175.04	0.24162	5.52
ACN650	650	252.95	0.3205	5.07

To further interpret the BET results, a comparison was made with selected studies reported in the literature. The surface area values obtained in this work fall within a wide range reported for biomass-derived carbon materials, where both preparation conditions and precursor type play a defining role. For instance, biochar derived from Phragmites australis in a previous study exhibited a surface area of 112.1 $m^2\ g^{-1}$ under multi-step thermal treatment up to 750 °C (Mortada et al., 2024), which is comparable to the values obtained in the present work at moderate temperatures. In contrast, biochar derived from water hyacinth showed a lower surface area of 50.54 $m^2\ g^{-1}$ at 400 °C (Xu et al., 2020), reflecting the influence of precursor composition and thermal severity.

A much lower surface area was reported for Acacia mangium at 500 °C (5.25 $m^2\ g^{-1}$) even in the presence of KOH activation (Danish et al., 2012), indicating that chemical activation alone does not guarantee high porosity without suitable structural characteristics of the raw material. On the other hand, extremely high surface area values, such as 907 $m^2\ g^{-1}$ for industrial cork activated with KOH at 800 °C, have been reported (Ullah et al., 2024), highlighting the strong effect of high activation temperature and optimized processing conditions.

The results of the present study show a clear increase in surface area with increasing temperature, particularly for activated samples, which can be attributed to the progressive development of pore structure during thermal treatment. Higher temperatures enhance the removal of volatile components and promote the formation of new pores. However, this improvement in textural properties is typically accompanied by a reduction in yield, as more carbon mass is lost during devolatilization and activation reactions.

In addition, parameters such as heating rate, activation duration, and type of activating agent significantly influence the final structure. Slower heating rates and longer residence times may allow more controlled pore development, while strong activating agents such as KOH contribute to pore widening and increased surface accessibility. Overall, the comparison confirms that the obtained results are consistent with reported trends, and that the balance between surface area development and yield loss is governed by the combined effect of temperature, activation conditions, and biomass characteristics.

4. Conclusions

The study showed that the plants Phragmites australis and water hyacinth possess primary properties that make them promising sources for producing versatile carbon materials, both in their bioactive and activated forms. The analysis revealed that the thermal response of the two plants differs significantly, directly impacting the mass yield and the porous structure formed at each stage of preparation.

In direct thermal decomposition, the mass yield gradually decreased with increasing temperature. However, this decrease was accompanied by a marked improvement in carbon content and structural stability, particularly in the Phragmites australis samples, which retained more uniform porosity at higher temperatures. These behaviors indicate that the dense fibrous structure of Phragmites australis with stands the temperature gradient better than that of water hyacinth, which loses mass rapidly due to its high water content and spongy structure, often resulting in lower surface areas in the resulting biochar.

However, when alkali activation with KOH was applied, the properties of the carbon material changed significantly. The alkaline reaction led to the opening of a large porous network in both materials, but the response of the water hyacinth was more pronounced. Sample ACN650 produced the highest surface area in the entire study, along with a significant increase in micropore size. This superiority reflects the ability of the water hyacinth's plant tissue to react deeply with the alkaline environment, allowing for the removal of a greater proportion of non-carbon components and a more extensive pore network than the activated reed under the same conditions.

In contrast, the activated reed retained good porous properties, but its structural development was minimal compared to the water hyacinth, indicating a fundamental difference in the mechanism of each plant's reaction to the activating agent. These results confirm that temperature control and the concentration of the activating agent are key factors in altering the nature of the carbon structure and directing it towards specific functions.

Overall, the study's findings demonstrate that the selection of the raw material is just as important as the manufacturing conditions, and that combining thermally controlled burning with chemical activation can produce high-specification carbon materials without the need for high-value plant sources. The outstanding performance of the ACN650 sample also highlights the potential for developing highly porous activated carbon from the abundant water hyacinth plant, opening up wide environmental and industrial applications, particularly in the fields of adsorption and water treatment.

5. Practical Recommendations

- To achieve the highest specific surface area and microporosity, it is preferable to treat the reed with KOH activation and a Pyrolysis temperature in the range of ~600–650 °C.
- For higher economic mass yield: It is recommended to operate at medium Pyrolysis temperatures (≈500–550 °C), especially for water hyacinth, and then perform moderate activation if increased porosity is required.
- Further analysis is required: Extract complete adsorption curves (isotherms) and analyze the tetrapore distribution (micropore vs. mesopore) and correlate them with the experimental adsorption performance of a specific pollutant (e.g., phenol or heavy metal ion) to confirm the material's suitability for the intended application. This step is essential for converting the methodological values (BET, pore sizes) into a true functional prediction of processing performance.

Acknowledgments

The authors sincerely thank the Baiji Oil Training Institute, affiliated with the Iraqi Ministry of Oil, for providing the opportunity to use its laboratory equipment.

References

Abdulrazzak, D. I. A. (2017). The effects of *Eichhornia crassipes* on the water resources. *The International Journal of Engineering and Science*, *06*(04), 51–55. https://doi.org/10.9790/1813-0604025155

Adesina, B. T., Okikiola, B. T., Elemile, O. O., Joseph, A., Dada, O. A., Obayomi, K. S., & Ajayi, O. E. (2021). Preparation and characterization of biochar and activated carbon derived from cashew bagasse waste. In ECS meeting abstracts (No. 60, p. 1770â). The Electrochemical Society. https://doi.org/10.1149/MA2021-02601770mtgabs

Ahmed, M. J. (2016). Application of agricultural based activated carbons by microwave and conventional activations for basic dye adsorption: Review. *Journal of Environmental Chemical Engineering*, *4*(1), 89–99. https://doi.org/10.1016/j.jece.2015.10.027

Ahmed, M. J., & Theydan, S. K. (2012). Physical and chemical characteristics of activated carbon prepared by pyrolysis of chemically treated date stones and its ability to adsorb organics. *Powder Technology*, *229*, 237–245. https://doi.org/10.1016/j.powtec.2012.06.043

Altenor, S., Carene, B., Emmanuel, E., Lambert, J., Ehrhardt, J. J., & Gaspard, S. (2009). Adsorption studies of methylene blue and phenol onto vetiver roots activated carbon prepared by chemical activation. Journal of Hazardous Materials, 165(1-3), 1029-1039. https://doi.org/10.1016/j.jhazmat.2008.10.133

Azargohar, R., & Dalai, A. K. (2006). Biochar as a precursor of activated carbon. Applied Biochemistry and Biotechnology, 131(1–

3), 762–773. https://doi.org/10.1385/ABAB:131:1:762

Azargohar, R., & Dalai, A. K. (2008). Steam and KOH activation of biochar: Experimental and modeling studies. *Microporous and Mesoporous Materials*, *110*(2–3), 413–421. https://doi.org/10.1016/j.micromeso.2007.06.047

Basta, A. H., Fierro, V., El-Saied, H., & Celzard, A. (2009). 2-Steps KOH activation of rice straw: An efficient method for preparing high-performance activated carbons. *Bioresource Technology*, *100*(17), 3941–3947. https://doi.org/10.1016/j.biortech.2009.02.028

Carneiro, M. T., Morais, A. Í. S., de Carvalho Melo, A. L. F., Ferreira, F. J. L., Santos, F. E. P., Viana, B. C., Osajima, J. A., Bezerra, R. D. S., Del Mar Orta Cuevas, M., Peña-Garcia, R. R., Almeida, L. C., & Silva-Filho, E. C. (2023). Biochar derived from water hyacinth biomass chemically activated for dye removal in aqueous solution. *Sustainability*, *15*(19), Article 14578. https://doi.org/10.3390/su151914578

Cazetta, A. L., Vargas, A. M. M., Nogami, E. M., Kunita, M. H., Guilherme, M. R., Martins, A. C., Silva, T. L., Moraes, J. C. G., & Almeida, V. C. (2011). NaOH-activated carbon of high surface area produced from coconut shell: Kinetics and equilibrium studies from the methylene blue adsorption. *Chemical Engineering Journal*, *174*(1), 117–125. https://doi.org/10.1016/j.cej.2011.08.058

Chambers, R. M., Meyerson, L. A., & Saltonstall, K. (1999). Expansion of *Phragmites australis* into tidal wetlands of north america. aquatic botany, *64*(3–4), 261–273. https://doi.org/10.1016/S0304-3770(99)00055-8

Chen, G., Bai, J., Yu, L., Wang, W., Wang, Y., Qiu, J., & Cui, B. (2024). *Phragmites australis* straw and biochar additives regulate soil organic carbon fractions in a degraded coastal salt marsh. *Ecological Engineering*, *206*, Article 107328. https://doi.org/10.1016/j.ecoleng.2024.107328

Colomba, A., Berruti, F., & Briens, C. (2022). Model for the physical activation of biochar to activated carbon. *Journal of Analytical and Applied Pyrolysis*, *168*, Article 105769. https://doi.org/10.1016/j.jaap.2022.105769

Danish, M., Hashim, R., Ibrahim, M. N. M., Rafatullah, M., & Sulaiman, O. (2012). Surface characterization and comparative adsorption properties of Cr(VI) on pyrolysed adsorbents of acacia mangium wood and phoenix dactylifera L. stone carbon. *Journal of Analytical and Applied Pyrolysis*, *97*, 19–28. https://doi.org/10.1016/j.jaap.2012.06.001

Elmouwahidi, A., Bailón-García, E., Pérez-Cadenas, A. F., Maldonado-Hódar, F. J., & Carrasco-Marín, F. (2017). Activated carbons from KOH and H_3PO_4 -activation of olive residues and its application as supercapacitor electrodes. *Electrochimica Acta*, *229*, 219–228. https://doi.org/10.1016/j.electacta.2017.01.152

Gale, M., Nguyen, T., Moreno, M., & Gilliard-AbdulAziz, K. L. (2021). Physiochemical properties of biochar and activated carbon from biomass residue: ınfluence of process conditions to adsorbent properties. *ACS Omega*, *6*(15), 10224–10233. https://doi.org/10.1021/acsomega.1c00530

Gaurav, G. K., Mehmood, T., Cheng, L., Klemeš, J. J., & Shrivastava, D. K. (2020). *Water hyacinth* as a biomass: A review. *Journal of Cleaner Production*, *277*, Article 122214. https://doi.org/10.1016/j.jclepro.2020.122214

Gong, Y.-P., Ni, Z.-Y., Xiong, Z.-Z., Cheng, L.-H., & Xu, X.-H. (2017). Phosphate and ammonium adsorption of the modified biochar based on *Phragmites australis* after phytoremediation. *Environmental Science and Pollution Research*, *24*(9), 8326–8335. https://doi.org/10.1007/s11356-017-8499-2

Hadey, C., Allouch, M., Alami, M., Boukhlifi, F., & Loulidi, I. (2022). Preparation and characterization of biochars obtained from biomasses for combustible briquette applications. *The Scientific World Journal*, *2022(1)*, 1–13. https://doi.org/10.1155/2022/2554475

Hagemann, N., Spokas, K., Schmidt, H.-P., Kägi, R., Böhler, M., & Bucheli, T. (2018). Activated carbon, biochar and charcoal: linkages and synergies across pyrogenic carbon's ABCs. *Water*, *10*(2), Article 182. https://doi.org/10.3390/w10020182

Harimisa, G. E., Jusoh, N. W. C., Tan, L. S., Shameli, K., Ghafar, N. A., & Masudi, A. (2022). Synthesis of potassium hydroxide-treated activated carbon via one-step activation method. *Journal of Physics: Conference Series*, *2259*(1), Article 012009. https://doi.org/10.1088/1742-6596/2259/1/012009

Al-Kinani, H. A., & Mana, H. A. (2025). Ecological and chemical study of *Eichhornia crassipes* plant growing in water of Shatt Al-Ksar in Thi-Qar-southern Iraq. University of Thi-Qar Journal of agricultural research, 14(1), 721-730. https://doi.org/10.54174/52jmm948

Huang, Y., Li, S., Chen, J., Zhang, X., & Chen, Y. (2014). Adsorption of Pb(II) on mesoporous activated carbons fabricated from water hyacinth using H_3PO_4 activation: Adsorption capacity, kinetic and isotherm studies. *Applied Surface Science*, *293*, 160–168. https://doi.org/10.1016/j.apsusc.2013.12.123

Hui, T. S., & Zaini, M. A. A. (2015). Potassium hydroxide activation of activated carbon: a commentary. *Carbon Letters*, *16*(4), 275–280. https://doi.org/10.5714/CL.2015.16.4.275

Hung, C.-M., Huang, C.-P., Hsieh, S.-L., Chen, Y.-T., Chen, C.-W., & Dong, C.-D. (2023). *Water hyacinth* derived biochar for polycyclic aromatic hydrocarbons removal and oxidative stress study. *Environmental Technology & Innovation*, *29*, Article 103027. https://doi.org/10.1016/j.eti.2023.103027

Jeirani, Z., Niu, C. H., & Soltan, J. (2017). Adsorption of emerging pollutants on activated carbon. *Reviews in Chemical Engineering*, *33*(5), 491–522. https://doi.org/10.1515/revce-2016-0027

Jiang, L., Chen, Y., Wang, Y., Lv, J., Dai, P., Zhang, J., Huang, Y., & Lv, W. (2022). Contributions of various Cd(II) adsorption mechanisms by phragmites australis -activated carbon modified with mannitol. *ACS Omega*, *7*(12), 10502–10515. https://doi.org/10.1021/acsomega.2c00014

Kassa, Y., Amare, A., Nega, T., Alem, T., Gedefaw, M., Chala, B., Freyer, B., Waldmann, B., Fentie, T., Mulu, T., Adgo, T., Ayalew, G., Adugna, M., & Tibebe, D. (2025). *Water hyacinth* conversion to biochar for soil nutrient enhancement in improving agricultural product. *Scientific Reports*, *15*(1), Article 1820. https://doi.org/10.1038/s41598-024-84729-x

Khalil, H. P. S., Jawaid, M., Firoozian, P., Rashid, U., Islam, A., & Akil, H. M. (2013). Activated carbon from various agricultural wastes by chemical activation with KOH: preparation and characterization. *Journal of Biobased Materials and Bioenergy*, *7*(6), 708–714.

Li, Z., Deng, H., Yang, L., Zhang, G., Li, Y., & Ren, Y. (2018). Influence of potassium hydroxide activation on characteristics and environmental risk of heavy metals in chars derived from municipal sewage sludge. *Bioresource Technology*, *256*, 216–223.

https://doi.org/10.1016/j.biortech.2018.02.013

Liao, Z., Huang, Z., Hu, H., Zhang, Y., & Tan, Y. (2011). Microscopic structure and properties changes of cassava stillage residue pretreated by mechanical activation. *Bioresource Technology*, *102*(17), 7953–7958. https://doi.org/10.1016/j.biortech.2011.05.067

Liu, P., Yue, M., & Zhang, H. (2016). Adsorptive performance of Ni(II) from aqueous solutions using biochar made of *Phragmites australis* by adding ammonium polyphosphate as flame retardant. *Journal of Chemistry*, *2016*(1), Article 1797396. https://doi.org/10.1155/2016/1797396

Ma, Y. (2017). Comparison of activated carbons prepared from wheat straw via ZnCl2 and KOH activation. *Waste and Biomass Valorization*, *8*(3), 549–559. https://doi.org/10.1007/s12649-016-9640-z

Madej, J., Hilber, I., Bucheli, T. D., & Oleszczuk, P. (2016). Biochars with low polycyclic aromatic hydrocarbon concentrations achievable by pyrolysis under high carrier gas flows irrespective of oxygen content or feedstock. *Journal of Analytical and Applied Pyrolysis*, *122*, 365–369. https://doi.org/10.1016/j.jaap.2016.09.005

Masto, R. E., Kumar, S., Rout, T. K., Sarkar, P., George, J., & Ram, L. C. (2013). Biochar from water hyacinth (*Eichornia crassipes*) and its impact on soil biological activity. *CATENA*, *111*, 64–71. https://doi.org/10.1016/j.catena.2013.06.025

Mortada, W. I., Ghaith, M. M., Khedr, N. E., Ellethy, M. I., Mohsen, A. W., & Shafik, A. L. (2024). Mesoporous magnetic biochar derived from common reed (Phragmites australis) for rapid and efficient removal of methylene blue from aqueous media. *Environmental Science and Pollution Research*, *31*(29), 42330–42341. https://doi.org/10.1007/s11356-024-33860-3

Najmudeen, T. M., Arakkal Febna, M. A., Rojith, G., & Zacharia, P. U. (2019). Characterisation of biochar from *Water Hyacinth Eichhornia crassipes* and the effects of biochar on the growth of fish and paddy in ıntegrated culture systems. *Journal of Coastal Research*, *86*(sp1), Article 225. https://doi.org/10.2112/SI86-033.1

Narayanan, M., Kandasamy, G., Kandasamy, S., Natarajan, D., Devarayan, K., Alsehli, M., Elfasakhany, A., & Pugazhendhi, A. (2021). Water hyacinth biochar and aspergillus niger biomass amalgamation potential in removal of pollutants from polluted lake water. *Journal of Environmental Chemical Engineering*, *9*(4), Article 105574. https://doi.org/10.1016/j.jece.2021.105574

Novotny, E. H., Maia, C. M. B. de F., Carvalho, M. T. de M., & Madari, B. E. (2015). Bıochar: Pyrogenıc carbon for agrıculturaL USE - A crıtıcal revıew. *Revista Brasileira de Ciência Do Solo*, *39*(2), 321–344. https://doi.org/10.1590/01000683rbcs20140818

Nwajiaku, I. M., Olanrewaju, J. S., Sato, K., Tokunari, T., Kitano, S., & Masunaga, T. (2018). Change in nutrient composition of biochar from rice husk and sugarcane bagasse at varying pyrolytic temperatures. *International Journal of Recycling of Organic Waste in Agriculture*, *7*(4), 269–276. https://doi.org/10.1007/s40093-018-0213-y

Okman, I., Karagöz, S., Tay, T., & Erdem, M. (2014). Activated carbons from grape seeds by chemical activation with potassium carbonate and potassium hydroxide. *Applied Surface Science*, *293*, 138–142. https://doi.org/10.1016/j.apsusc.2013.12.117

Orero, B., Ntuli, F., Zvinowanda, C., Sithole, T., & Mashifana, T. (2025). Sustainable synthesis of activated carbon from water hyacinth via one-step carbonization-H_3PO_4 activation: Optimization and modeling via RSM-artificial intelligence approach. *Next Materials*, *9*, Article 101140. https://doi.org/10.1016/j.nxmate.2025.101140

Ouyang, J., Zhou, L., Liu, Z., Heng, J. Y., & Chen, W. (2020). Biomass-derived activated carbons for the removal of pharmaceutical mircopollutants from wastewater: A review. Separation and Purification Technology, 253, Article 117536. https://doi.org/10.1016/j.seppur.2020.117536

Patnukao, P., & Pavasant, P. (2008). Activated carbon from Eucalyptus camaldulensis Dehn bark using phosphoric acid activation. *Bioresource Technology*, *99*(17), 8540–8543. https://doi.org/10.1016/j.biortech.2006.10.049

De Araújo, T. P., Quesada, H. B., Bergamasco, R., Vareschini, D. T., & De Barros, M. A. S. D. (2020). Activated hydrochar produced from brewer's spent grain and its application in the removal of acetaminophen. Bioresource Technology, 310, Article 123399. https://doi.org/10.1016/j.biortech.2020.123399

Reddy, K. S. K., Al Shoaibi, A., & Srinivasakannan, C. (2012). A comparison of microstructure and adsorption characteristics of activated carbons by CO_2 and H_3PO_4 activation from date palm pits. *New Carbon Materials*, *27*(5), 344–351. https://doi.org/10.1016/S1872-5805(12)60020-1

Rezania, S., Ponraj, M., Talaiekhozani, A., Mohamad, S. E., Md Din, M. F., Taib, S. M., Sabbagh, F., & Sairan, F. M. (2015). Perspectives of phytoremediation using water hyacinth for removal of heavy metals, organic and inorganic pollutants in wastewater. *Journal of Environmental Management*, *163*, 125–133. https://doi.org/10.1016/j.jenvman.2015.08.018

Riyanto, C. A., & Prabalaras, E. (2019). The adsorption kinetics and isoterm of activated carbon from *Water hyacinth* leaves (*Eichhornia crassipes*) on Co(II). *Journal of Physics: Conference Series*, *1307*(1), Article 012002. https://doi.org/10.1088/1742-6596/1307/1/012002

Rolletschek, H., Rolletschek, A., Kühl, H., & Kohl, J.-G. (1999). Clone specific differences in a *Phragmites australis* stand. *Aquatic Botany*, *64*(3–4), 247–260. https://doi.org/10.1016/S0304-3770(99)00054-6

Saad, M. J., Sajab, M. S., Wan Busu, W. N., Misran, S., Zakaria, S., Chin, S. X., & Chia, C. H. (2020). Comparative adsorption mechanism of rice straw activated carbon activated with NaOH and KOH. *Sains Malaysiana*, *49*(11), 2721–2734. https://doi.org/10.17576/jsm-2020-4911-11

Salman, S. D., Rasheed, I. M., & Mohammed, A. K. (2021). Adsorption of heavy metal ions using activated carbon derived from Eichhornia (water hyacinth). *IOP Conference Series: Earth and Environmental Science*, *779*(1), Article 12074. https://doi.org/10.1088/1755-1315/779/1/012074

Saltonstall, K. (2002). Cryptic invasion by a non-native genotype of the common reed, *Phragmites australis* , into north america. *Proceedings of the National Academy of Sciences*, *99*(4), 2445–2449. https://doi.org/10.1073/pnas.032477999

Sharifirad M, Koohyar F, Rahmanpour SH, & Vahidifar M. (2012). Preparation of activated carbon from *Phragmites Australis*: Equilibrium Behaviour Study. *Research Journal of Recent Sciences*, *1*(8), 10–16. https://www.isca.me/rjrs/archive/v1/i8/2.ISCA-RJRS-2012-167.pdf

Shengli, S., Junping, L., Qi, L., Fangru, N., Jia, F., & Shulian, X. (2018). Optimized preparation of *Phragmites australi*s activated carbon using the box-behnken method and desirability function to remove hydroquinone. *Ecotoxicology and Environmental Safety*, *165*, 411–422. https://doi.org/10.1016/j.ecoenv.2018.09.038

Tarapitakcheevin, P., Weerayutsil, P., & Khuanmar, K. (2013). Adsorption of acid dye on activated carbon prepared from *Water*

Hyacinth by sodium chloride activation. GMSARN International Journal, 7(1), 83-90. https://gmsarnjournal.com/home/wp-content/uploads/2015/08/vol7no3-1.pdf

Thompson, K. A., Shimabuku, K. K., Kearns, J. P., Knappe, D. R. U., Summers, R. S., & Cook, S. M. (2016). Environmental Comparison of biochar and activated carbon for tertiary wastewater treatment. *Environmental Science & Technology*, *50*(20), 11253–11262. https://doi.org/10.1021/acs.est.6b03239

Toft, J. D., Simenstad, C. A., Cordell, J. R., & Grimaldo, L. F. (2003). The effects of introduced water hyacinth on habitat structure, invertebrate assemblages, and fish diets. *Estuaries*, *26*(3), 746–758. https://doi.org/10.1007/BF02711985

Tseng, R., & TSENG, S. (2006). Characterization and use of high surface area activated carbons prepared from cane pith for liquid-phase adsorption. *Journal of Hazardous Materials*, *136*(3), 671–680. https://doi.org/10.1016/j.jhazmat.2005.12.048

Ullah, S., Shah, S. S. A., Altaf, M., Hossain, I., El Sayed, M. E., Kallel, M., El-Bahy, Z. M., Rehman, A. ur, Najam, T., & Nazir, M. A. (2024). Activated carbon derived from biomass for wastewater treatment: Synthesis, application and future challenges. *Journal of Analytical and Applied Pyrolysis*, 179, Article 106480. https://doi.org/10.1016/j.jaap.2024.106480

Wang, W., Bai, J., Lu, Q., Zhang, G., Wang, D., Jia, J., Guan, Y., & Yu, L. (2021). Pyrolysis temperature and feedstock alter the functional groups and carbon sequestration potential of Phragmites australis - and Spartina alterniflora -derived biochars. *GCB Bioenergy*, *13*(3), 493–506. https://doi.org/10.1111/gcbb.12795

Williams, N. E., Oba, O. A., & Aydinlik, N. P. (2022). Modification, production, and methods of KOH-activated carbon. *ChemBioEng Reviews*, *9*(2), 164–189. https://doi.org/10.1002/cben.202100030

Xiao, H., Lin, Q., Li, G., Zhao, X., Li, J., & Li, E. (2022). Comparison of biochar properties from 5 kinds of halophyte produced by slow pyrolysis at 500 °C. *Biochar*, *4*(1), Article 12. https://doi.org/10.1007/s42773-022-00141-6

Xu, Z., Xing, Y., Ren, A., Ma, D., Li, Y., & Hu, S. (2020). Study on adsorption properties of water hyacinth-derived biochar for uranium (VI). *Journal of Radioanalytical and Nuclear Chemistry*, *324*(3), 1317–1327. https://doi.org/10.1007/s10967-020-07160-2

Zhang, C., Shao, Y., Zhang, L., Zhang, S., Westerhof, R. J. M., Liu, Q., Jia, P., Li, Q., Wang, Y., & Hu, X. (2020a). Impacts of temperature on evolution of char structure during pyrolysis of lignin. *Science of The Total Environment*, *699*, Article 134381. https://doi.org/10.1016/j.scitotenv.2019.134381

Zhang, C., Zhang, Z., Zhang, L., Li, Q., Li, C., Chen, G., Zhang, S., Liu, Q., & Hu, X. (2020b). Evolution of the functionalities and structures of biochar in pyrolysis of poplar in a wide temperature range. *Bioresource Technology*, *304*, Article 123002. https://doi.org/10.1016/j.biortech.2020.123002

Zhang, Y.-Y., Zhang, D., & Barrett, S. C. H. (2010). Genetic uniformity characterizes the invasive spread of water hyacinth (*Eichhornia crassipes*), a clonal aquatic plant. *Molecular Ecology*, *19*(9), 1774–1786. https://doi.org/10.1111/j.1365-294X.2010.04609.x

Zhao, C., Yin, W., Xu, J., Zhang, Y., Shang, D., Guo, Z., Wang, Q., Wang, J., & Kong, Q. (2020). Removal of tetracycline from water using activated carbon derived from the mixture of *Phragmites australis* and waterworks sludge. *ACS Omega*, *5*(26), 16045–16052. https://doi.org/10.1021/acsomega.0c01524